



# HHS Public Access

Author manuscript

*Nat Methods*. Author manuscript; available in PMC 2014 April 01.

Published in final edited form as:

*Nat Methods*. 2013 October ; 10(10): 992–995. doi:10.1038/nmeth.2605.

## Renewable, recombinant antibodies to histone post-translational modifications

Takamitsu Hattori<sup>1</sup>, Joseph M. Taft<sup>1</sup>, Kalina M. Swist<sup>1,2</sup>, Hao Luo<sup>3</sup>, Heather Witt<sup>4</sup>, Matthew Slattery<sup>5,6</sup>, Akiko Koide<sup>1</sup>, Alexander J. Ruthenburg<sup>1,7</sup>, Krzysztof Krajewski<sup>8</sup>, Brian D. Strahl<sup>8</sup>, Kevin P. White<sup>5,6</sup>, Peggy J. Farnham<sup>4</sup>, Yingming Zhao<sup>3</sup>, and Shohei Koide<sup>1</sup>

<sup>1</sup>Department of Biochemistry and Molecular biology, The University of Chicago, Chicago, IL, USA

<sup>2</sup>Department of Biochemistry, Wrocław University of Technology, Wrocław, Poland <sup>3</sup>Ben May Department of Cancer Research, The University of Chicago, Chicago, IL, USA <sup>4</sup>Department of Biochemistry and Molecular Biology, Norris Comprehensive Cancer Center, University of Southern California, Los Angeles, CA, USA <sup>5</sup>Institute for Genomics and Systems Biology, The University of Chicago, Chicago, IL, USA <sup>6</sup>Department of Human Genetics, The University of Chicago, Chicago, IL, USA <sup>7</sup>Department of Molecular Genetics and Cell Biology, The University of Chicago, Chicago, IL, USA <sup>8</sup>Department of Biochemistry and Biophysics, University of North Carolina School of Medicine, Chapel Hill, NC, USA

### Abstract

Variability in the quality of antibodies to histone post-translational modifications (PTMs) presents widely recognized hindrance in epigenetics research. Here, by using antibody engineering technologies we produced recombinant antibodies directed to the trimethylated lysine residues of histone H3 with high specificity and affinity and no lot-to-lot variation. These recombinant antibodies performed well in common epigenetics applications, and their high specificity enabled us to identify positive and negative correlations among histone PTMs.

Post-translational modifications (PTMs) of histone proteins play key roles in epigenetics regulation<sup>1,2</sup>. Antibodies to histone PTMs are critical components in epigenetics investigation such as chromatin immunoprecipitation (ChIP), immunostaining and immunoblotting<sup>3,4</sup>, but many antibodies to histone PTMs fail to specifically recognize their intended targets<sup>5–7</sup>. Furthermore, currently available anti-histone antibodies are mostly

Users may view, print, copy, download and text and data- mine the content in such documents, for the purposes of academic research, subject always to the full Conditions of use: [http://www.nature.com/authors/editorial\\_policies/license.html#terms](http://www.nature.com/authors/editorial_policies/license.html#terms)

Correspondence and material requests should be addressed to S.K. (skoide@uchicago.edu).

#### Author contributions

T.H. characterized commercial antibodies; T.H., A.K. and S.K. designed phage-display libraries and selection schemes; T.H., J.T. and K.S. performed selections and biophysical characterization of recombinant antibodies; K.K. and B.D.S. designed and made synthetic peptides; T.H., H.W., M.S., A.J.R., K.P.W., P.J.F. and S.K. designed ChIP experiments; T.H., H.W. and M.S. conducted ChIP experiments and data analysis; T.H., H.L., Y.Z. and S.K. designed IP-MS experiments; T.H. and H.L. performed IP-MS and data analysis; T.H. and S.K. designed HMT assay; T.H. conducted HMT assay. T.H. and S.K. wrote the manuscript. All authors commented on the manuscripts.

Competing financial statement: TH, JMT, AK and SK are named as inventors in a provisional patent application filed by the University of Chicago on the described materials.

polyclonal, and hence each lot of antibody is a different product that needs to be extensively validated prior to use. Thus, these issues impose a substantial burden of both time and expense on individual investigators.

Here, we sought to generate high-quality recombinant antibodies to histone PTMs to address this “antibody bottleneck”. We concentrated our initial efforts in obtaining high-quality anti-H3K9me3 antibodies, because of our difficulty in identifying such antibodies. We recently established a quantitative peptide immunoprecipitation (IP) assay that determines the dissociation constant ( $K_D$ ), the fundamental parameter defining affinity and specificity, and characterized a panel of commercial antibodies<sup>7</sup>. We identified an excellent anti-H3K4me3 antibody, but all anti-H3K9me3 antibodies (two polyclonal and one monoclonal antibodies) tested exhibited poor quality<sup>7</sup>. Thus, we expanded our survey of anti-H3K9me3 antibodies. The affinity, specificity and binding capacity of commercial anti-H3K9me3 antibodies varied greatly (Fig. 1a, Supplementary Fig. 1). Of eight antibodies, including those reported previously<sup>7</sup>, only a polyclonal antibody, pAb-056-050 (lot A93-0042), showed high affinity to H3K9me3 and almost no cross-reactivity to the other peptides, indicating excellent quality. Unfortunately, this lot is no longer available, and another lot of the same product showed distinct and lower quality than the first, indicating substantial lot-to-lot variation (Fig. 1a). Histone PTMs are challenging targets for antibody recognition, because the chemical differences among PTMs are minute, in particular among methylation states, and because there is a high level of sequence similarity surrounding the different modification sites. Furthermore, it is difficult to achieve high affinity to a flexible peptide, such as histone tails, due to a large entropic loss associated with binding<sup>8</sup>. Consequently, the difficulty in generating high-quality antibodies, regardless of antibody generation methods, is not unexpected.

We first identified, from a human naïve antibody library<sup>9</sup>, a single chain Fv (scFv) clone, termed “scFv4-5”, that bound to trimethylated Lys with high specificity but low affinity and low sequence specificity (Supplementary Fig. 2a-2c). To improve the binding function, we identified positions that are important for recognition of trimethylated Lys using shotgun-scanning mutagenesis<sup>10</sup> (Supplementary Fig. 2d,e). We then designed and sorted a second-generation phage-display library. Candidate clones were converted into the Fab format (Supplementary Fig. 2b), expressed in *E. coli*, purified, and characterized using the peptide IP assay. One clone, termed 309M3-A, had a  $K_D$  of 24 nM to H3K9me3, representing ~80 fold improvement from scFv4-5, and almost no binding to the other peptides tested, indicating both high affinity and high specificity (Fig. 1b, Supplementary Fig. 3a,b). Importantly, two independent preparations of the 309M3-A antibody showed no significant lot-to-lot variation (Supplementary Fig. 3a). Furthermore, its binding capacity, defined as the amount of peptide that an equivalent amount of an antibody captures, was higher than most of polyclonal anti-H3K9me3 antibodies including pAb-056-050 (lot A93-0042), the best commercial antibody we found (Supplementary Fig. 3c). We also designed a non-functional antibody, termed “NegM3”, by mutating four residues of scFv4-5. This should be a more appropriate control for identifying background effects from the antibody framework than generic “IgG controls” of unknown properties that are often used in ChIP experiments. As demonstrated here, the iterative process of designing a library and characterizing

antibodies can produce highly functional antibodies. Such improvement is nearly impossible for conventional polyclonal and monoclonal antibodies, illustrating a clear advantage of recombinant antibodies.

Although antibodies to histone PTMs are often influenced by combinatorial PTMs adjacent to their targeted mark<sup>11</sup>, remarkably, our 309M3-A antibody was generally insensitive to neighboring modifications. Modifications at K4, T6, R8 or S10 resulted in only small changes in affinity of 309M3-A (Fig. 1c). In contrast, a single secondary modification reduced the affinity of pAb-056-050 (lot A93-0042) by >50 fold (Fig. 1c), suggesting that this antibody achieves its high functionality by recognizing features over several residues surrounding H3K9me3. Thus, 309M3-A is a suitable reagent for capturing histones containing the H3K9me3 mark without a strong bias in terms of adjacent modifications.

The 309M3-A antibody specifically recognized full-length histone H3 from human cell lines (Supplementary Fig. 3d). Immunostaining of NIH 3T3 cells with it yielded a punctate pattern where the foci overlapped with those of the fluorochrome 4',6'-diamidino-2-phenylindole (DAPI) staining (Fig. 1e). This pattern indicated that 309M3-A staining was concentrated in the pericentric heterochromatin regions, regions enriched with H3K9me3<sup>12</sup>, suggesting that 309M3-A recognizes the H3K9me3 in the nucleus.

In addition to anti-H3K9me3 antibodies, we successfully developed anti-H3K4me3 antibodies. One clone, named 304M3-A, exhibited a  $K_D$  value of 16 nM to H3K4me3 with high specificity and no significant lot-to-lot variation (Supplementary Fig. 4a,b). The affinity of 304M3-A was negatively affected by PTMs of R2, T3, T6 and the N-terminal backbone amine (Supplementary Fig. 4c), indicating that this antibody, unlike 309M3-A, achieves specificity by recognizing features spanning the N-terminus to residue 6. Together, these results strongly suggest the feasibility of generating high-quality recombinant antibodies to a range of histone PTMs.

As ChIP is arguably the most important application of anti-histone PTM antibodies, we tested our recombinant antibodies in a series of ChIP experiments. ChIP from HEK293 cells with 309M3-A and 304M3-A respectively enriched specific loci marked with H3K9me3 and H3K4me3, 3' ends of ZNFs and HOXA9/GAPDH<sup>13, 14</sup> (Fig. 2a). In contrast, the negative control antibody, whose Fv portion differs from the lead antibody, scFv4-5, by only four residues, enriched none of these loci, indicating low background binding of the antibody framework. Although ChIP from HEK293T cells with 309M3-A and pAb-056-050 (lot A93-0042) showed similar profiles in ChIP-qPCR and ChIP-Seq, 309M3-A gave higher enrichment (Supplementary Fig. 5a,b). This difference in enrichment is consistent with the difference in binding capacity of the two antibodies revealed in the peptide IP assay (Supplementary Fig. 3c). Finally, ChIP-seq data of *D. melanogaster* embryos showed highly correlated peak patterns between biological replicates, indicating high reproducibility (Fig. 2b). Together, these data demonstrated that the recombinant antibodies performed well in ChIP experiments with a variety of chromatin samples.

To further examine the specificity and utility of 309M3-A, we performed immunoprecipitation (IP) followed by mass spectrometry (MS), which directly quantifies

histone modifications<sup>15</sup> (Supplementary Fig. 6a). IP with 309M3-A from GluC-digested histone H3 highly enriched H3K9me3 (from 23% to 79%) and depleted H3K9me2, the most abundant mark identified for H3K9 (from 45% to 8%) (Fig. 2c), confirming that 309M3-A selectively enriched histone fragments containing H3K9me3. Although R8 modifications slightly increased the affinity of 309M3-A to H3K9me3 (Fig. 1c), we did not observe enrichment of a peptide containing H3K9me3 and R8 modification, suggesting that the IP efficiency was not strongly biased by secondary modifications. IP-MS also enables us to determine combinatorial histone PTMs residing in the same histone tail. We found that 25% of captured peptides containing H3K9me3 also had H3K14Ac (Supplementary Fig. 6b), indicating these two marks often coexist. Interestingly, trimethylation at K27 increased 3-fold after IP (Fig. 2c and Supplementary Fig. 6c,d). Because 309M3-A exhibited no detectable binding to the H3K27me3 peptide (Fig. 1b), these data suggest that H3K9me3 partially coexisted with H3K27me3. In contrast, H3K36me2 was dramatically decreased after IP, indicating negative correlation between H3K9me3 and H3K36me2 (Fig. 2c and Supplementary Fig. 6c,d). This negative correlation could be deduced from the positive correlation between H3K9me3 and H3K27me3 as described above and negative correlation between H3K27me2/me3 and H3K36me2/me3 reported recently<sup>16</sup>. Together, the high specificity of the recombinant antibody enabled us to identify both positive and negative correlations among histone PTMs.

Finally, we exploited the high specificity and renewability of 309M3-A to develop an assay for histone methyltransferase (HMT) activity. HMT and histone demethylase are emerging drug targets<sup>17</sup>, but low specificity of antibodies is a serious impediment to developing antibody-based screening assays for these enzymes<sup>18</sup>. We first evaluated our recombinant antibody and commercial antibodies for their ability to discriminate H3K9me2 and H3K9me3. 309M3-A showed a large dynamic range and identical profiles between two lots, much superior to a polyclonal antibody, Ab8898 (Fig. 2d). This assay with 309M3-A clearly detected SUV39H1 activity and its inhibition by chaetocin<sup>17</sup> (Fig. 2e). These results illustrate that the high specificity and consistent quality of recombinant antibodies are ideally suited for developing HMT assays.

The truly renewable nature of recombinant antibodies justifies efforts and expenses for comprehensive validation, which liberates individual investigators from the need for evaluating each antibody. Recombinant antibodies can be further engineered into different formats suitable for particular applications. An intriguing possibility is the development of "intrabodies", that is intracellularly expressed antibodies, for real-time detection and perturbation of intracellular events<sup>19</sup>. Thus, recombinant anti-histone PTM antibodies can not only dramatically accelerate and improve the quality of epigenetics research but also enable new investigations.

## Online Methods

### Peptides and commercial antibodies

Peptide sequences are given in Supplementary Fig. 1a. Synthetic peptides were purchased from Abgent and Genemed Synthesis, or synthesized in-house<sup>11</sup>. Peptides were biotinylated as described previously<sup>7</sup>. Antibodies were purchased from their respective vendors.

## Peptide IP assay

For commercial antibodies, 100  $\mu$ L of protein A or protein G-coated polystyrene beads (Spherotech Inc.) and 1  $\mu$ g of an antibody sample were incubated for 1 hr at 4°C to prepare antibody-coated beads. For recombinant antibodies, which were produced in the form of biotinylated Fab, 100  $\mu$ L of streptavidin-coated polystyrene beads (Spherotech Inc.) and 0.6  $\mu$ g of a biotinylated Fab sample (equivalent to 1  $\mu$ g of IgG antibody) were incubated and then excess biotin-binding sites of streptavidin were blocked with biotin. These antibody-coated beads were used for the assay as described previously<sup>7</sup>.

Although it is technically true that the assay measures the combined strength of all interactions involved (sometimes called "avidity"), in practice the assay essentially measures the affinity of the interaction between an antibody and a peptide. The  $K_D$  values for the interaction of Protein A with rabbit IgG (or Protein G with mouse IgG) are in the single nanomolar or sub-nanomolar range<sup>20</sup>, much lower than the "net  $K_D$ " values that we found for the antibody-peptide interactions in the assay. Therefore, these results indicate that the contribution of the interaction between Protein A/G and IgG to the determined  $K_D$  value is negligible and that our assay effectively analyzes the interaction between antibody and peptide. Likewise, the interaction between biotin and streptavidin is extremely tight, and thus the assay for biotinylated Fab measures the affinity of the antibody-peptide interaction.

## In vitro selection of recombinant antibodies

Selection of recombinant antibodies from a human naïve library using yeast display was performed as described<sup>21</sup>, except that the first round of selection was performed using antigen-coated magnetic beads as previously described<sup>22</sup>. Biotinylated peptides were used as antigen (Supplementary Fig. 1a). In the first round, streptavidin magnetic beads were first incubated with excess amounts of a biotinylated peptide and used for selection. In the second round, a biotinylated peptide at 2  $\mu$ M was used for library sorting using FACS.

A phage display vector of scFv4-5 was constructed by cloning the DNA encoding the scFv segment in the DsbFNp3FL vector<sup>23</sup>. This vector displays the scFv on the surface of M13 bacteriophage as a fusion protein to the C-terminal domain of the M13 p3 coat protein. Shotgun-scanning mutagenesis analysis was performed following the method of Weiss et al.<sup>10</sup> Residues in the complementarity determining regions (CDRs) were diversified with a binary choice of the wild-type amino acid and either Ser or Ala. When such a binary code cannot be encoded using a "wobble" codon, a codon encoding four amino acids was used. Specifically, codons and encoded amino acids used here are: KCT (K = G or T) for Ala or Ser; GMT (M = A or C) for Asp or Ala; TYT (Y = C or T) for Phe or Ser; GST (S = C or G) for Gly or Ala; MRT (R = A or G) for His, Ser, Arg or Asn; AKT for Ile or Ser; RMA for Lys, Ala, Thr or Glu; TYG for Leu or Ser; RYG for Met, Ala, Thr or Val; ART for Asn or Ser; MCT for Pro or Ala; SMA for Gln, Ala, Pro or Glu; AGW (W = A or T) for Arg or Ser; RCT for Thr or Ala; GYT for Val or Ala; TSG for Trp or Ser; TMT for Tyr or Ser. The ratio of the wild type amino acid over a replacement at each mutated position was determined for recovered clones that retained binding to H3K4me3 or H3K9me3 by DNA sequencing.

A second-generation phage-display library was constructed based on analysis of shotgun-scanning mutagenesis, in which residues in the CDRs of scFv4-5 were randomized. This library was subjected to selection for binding to H3K9me3 or H3K4me3 peptides that also include negative selection against other peptides, essentially following published methods<sup>24</sup>. A biotinylated peptide at 100 nM was used for selections. Clones that had high specificity were identified by phage ELISA analysis.

### Expression and purification of recombinant antibodies

scFv clones were reformatted into the Fab form using an expression vector previously described<sup>25</sup>. Here, the C<sub>H1</sub> and C<sub>L</sub> portions of the 4D5 antibody were attached to the V<sub>H</sub> and V<sub>L</sub> portions, respectively, derived from scFv clones. The antibodies additionally contained a biotinylation acceptor peptide at the C-terminus of the heavy chain. The antibodies were expressed in *E. coli* 55244 (ATCC) harboring a plasmid that coexpressed the BirA biotin ligase in media supplemented with biotin. Fab samples were loaded on a HiTrap Protein G HP column (GE Healthcare) using 20 mM sodium phosphate buffer and eluted with 0.1 M Gly-HCl (pH 2.7). The eluted Fab samples were further purified on a Resource S column (GE Healthcare) using a linear gradient of NaCl in 50 mM sodium acetate buffer (pH 5.0). Purity was verified by SDS-PAGE.

### Western blot analysis

The K562 cells were grown in the RPMI 1640 media (Gibco) with 2 mM L-glutamine, 10% fetal bovine serum (FBS) and antibiotics. Whole cell extracts of K562 cells ( $1 \times 10^6$ ) were separated using SDS-PAGE and blotted to a nitrocellulose membrane. The membrane was blocked with PBST buffer (PBS and 0.05% Tween 20) containing 5% skim milk and rinsed with PBST buffer. The membrane was probed with 309M3-A or commercial antibodies in PBST containing 1% BSA using a multi-channel Western blotting apparatus (Idea Scientific Company). The 309M3-A antibody was detected with horseradish peroxidase (HRP) conjugated neutravidin (Pierce) and polyclonal antibodies were detected with goat anti-rabbit IgG-HRP (Pierce).

### Immunofluorescence analysis

The NIH 3T3 cells were grown in the DMEM (Cellgro) media with 2 mM L-glutamine, 10% FBS and antibiotics. Immunofluorescence analysis was performed as described<sup>26</sup>. The rabbit polyclonal antibody was detected with Dylight650 conjugated anti-rabbit polyclonal antibody (Pierce). The recombinant antibodies were first mixed with Dylight650-conjugated streptavidin (Pierce) at a molar ratio of 4:1 to form antibody-streptavidin complexes. After 30 min incubation at 4°C, excess biotin-binding sites of streptavidin were blocked with biotin, and then the antibody-streptavidin complexes were used in staining of the cells.

### Native ChIP followed by qPCR

Native ChIP experiments using HEK293 cells were performed as previously described<sup>27</sup> with the following modifications. Micrococcal nuclease-digested nuclei from HEK293 cells were purified using hydroxyapatite chromatography with stepwise elution in 50, 100, 200 and 500 mM sodium phosphate buffer (pH 7.2) containing 100 mM NaCl, 1 mM EDTA and

200  $\mu$ M PMSF. The purity of nucleosomes in elution fractions was examined by SDS-PAGE and high-purity fractions were used for ChIP. Streptavidin MagneSphere paramagnetic particles (Promega) were washed twice with TBS containing 0.5% BSA, and mixed with a biotinylated recombinant antibody. After 1 hr incubation at 4°C, excess biotin-binding sites of streptavidin were blocked with biotin, and then beads were washed twice with IP buffer (83 mM sodium phosphate (pH7.2) buffer containing 100 mM KCl, 2 mM MgCl<sub>2</sub>, 10% v/v glycerol, 0.1% v/v NP-40, 200  $\mu$ M PMSF and protease inhibitor cocktail (Roche)). See Supplementary Note for a protocol for preparing Fab-loaded magnetic beads. Five  $\mu$ g of purified nucleosomes was incubated with 1.7  $\mu$ g of Fab (equivalent to 2.5  $\mu$ g of IgG) immobilized on beads for overnight at 4°C. Otherwise, washing, elution and DNA purification were performed as described<sup>27</sup>. Primers used for qPCR have been described previously<sup>27, 28</sup>.

### Cross-linked ChIP from HEK293T cells followed by qPCR and sequencing

The HEK293T cells were grown in the DMEM (Cellgro) media with 2 mM L-glutamine, 10% FBS and antibiotics. The cells were treated with 5  $\mu$ M 5-azacytidine for 8 days, with the medium changed daily. Cross-linked ChIP experiments from HEK293T cells were performed as described<sup>29</sup> with the following modifications. For ChIP assays using a recombinant antibody, 1.3  $\mu$ g of Fab (equal to 2  $\mu$ g amount of IgG) immobilized on beads was prepared as described above, and incubated with 20  $\mu$ g of chromatin. For ChIP assays using the commercial antibody, 2  $\mu$ g and 8  $\mu$ g of anti-H3K9me3 polyclonal antibody, pAb-056-050 (lot A93-0042, Diagenode), were used for ChIP-qPCR and ChIP-seq, respectively. After confirming enrichment of target sequences in ChIP versus input samples using qPCR, libraries were created as previously described with minor modifications<sup>29</sup>. Gel size selection of the 200–500 bp fraction was conducted after the adapter ligation step, followed by 10–15 amplification cycles. The libraries were analyzed using an Illumina GAIIx. Sequence reads were aligned to the UCSC human genome assembly HG19 using the Eland pipeline (Illumina). Primers used for qPCR were previously described<sup>28</sup>.

### Cross-linked ChIP from embryos of *D. melanogaster* followed by sequencing

Cross-linked ChIP experiments from *D. melanogaster* were performed essentially as described previously<sup>30</sup>. The 309M3-A antibody (3.3  $\mu$ g; equivalent to 5  $\mu$ g IgG) was immobilized onto magnetic beads as described above, and incubated overnight at 4°C with sonicated cross-linked chromatin extract from 100 mg of whole *D. melanogaster* embryos (0–8 hour embryos). Immunoprecipitated DNA was prepared for sequencing using the Epicentre Nextera DNA Sample Preparation Kit. Library preparation was performed using the High Molecular Weight tagmentation buffer, and tagmented DNA was amplified using 12 cycles of PCR. Library DNA was then sequenced on an Illumina HiS eq 2000 according to the manufacturer's standard protocols. Sequences were aligned to the Drosophila genome using BWA; properly aligned reads with mapping quality greater than 30 were kept.

### IP followed by MS analysis

Nucleosome samples contain fragments larger than the mono-nucleosome (e.g. di- and tri-nucleosomes) and the mono-nucleosome contains two copies of each histone protein.

Consequently, it is challenging to determine whether an identified PTM is present in the protein molecule that is directly captured by an antibody or in the other molecules within the same captured chromatin fragment. Similarly, it is difficult to determine whether or not additional PTMs reside on the same histone molecule. To minimize this ambiguity, we purified and proteolytically cleaved histone H3 with endoproteinase GluC to produce a monomeric peptide spanning residues 1–50, and used the digest as the input for IP, instead of nucleosomes or entire histone proteins.

Acid extracted histones from HeLa cells were prepared as previously described<sup>31</sup>. Acid extracted histones from HeLa cells were separated on a Vydac 214TP C4 reversed phase column (150 mm × 4.6mm ID, 5 μm particle, 300Å pore size, Grace) using a gradient of acetonitrile in 0.1 % TFA. After lyophilization, the histone H3 sample was digested with endoproteinase GluC (Roche) with an enzyme to protein ratio of 1: 50 in 100 mM ammonium acetate buffer (pH 4.0) for 4 hr at 37 °C. Immunoprecipitation with the 309M3-A antibody was performed as described above under "Native CHIP followed by qPCR", except that the incubation period was 2 hr. After washing the beads, bound peptides were eluted with 0.1% TFA in water. Propionylation of peptides was performed as described<sup>32</sup>. The input and immunoprecipitated peptides were propionylated using <sup>12</sup>C- or <sup>13</sup>C- propionic anhydride. Samples were lyophilized, dissolved in 50 mM NH<sub>4</sub>HCO<sub>3</sub> (pH 8.0) and digested with trypsin. The newly generated N-terminal amine group of the digested peptides was also propionylated. Samples were lyophilized and dissolved in 0.1% formic acid. The digested peptide mixtures from the input and IP pools were mixed in such a way that the total spectral counts for the two pools were approximately equal, and the mixture was subjected to mass spectrometry analysis.

HPLC/MS/MS experiments and data analysis were performed as previously described<sup>15</sup>. The peptides were separated by HPLC (Eksigent Technologies) before analyzed by an LTQ-Orbitrap Velos mass spectrometer (Thermo Fisher Scientific). The molecular masses of peptides were determined with a precision of ±0.02 by high resolution Orbitrap mass analyzer, and their MS/MS spectra were generated in the data-dependent mode. The collected MS/MS spectra were searched against the human protein sequence database using Mascot. The spectral counting method was used to quantify the enrichment of the modified peptides. The percentage of the spectral count for a peptide containing the modification of interest to the sum of the spectral counts for all peptides containing the residue harboring the modification of interest, was calculated. The quantification experiments were carried out twice.

### Histone methyltransferase (HMT) assay

ELISA experiments were performed as follows. The wells of 96-well plates (Greiner Bio-One) were coated with neutravidin (Pierce) and blocked with BSA. Biotinylated peptides were added to the wells and excess biotin-binding sites of immobilized neutravidin were blocked with biotin. After washing with the TBST buffer, the bound peptides were detected with 309M3-A or Ab8898 followed by HRP-conjugated neutravidin (Pierce) or HRP-conjugated goat anti-rabbit antibody (Pierce), respectively.



For HMT assay, 400 nM of SUV39H1 (Reaction Biology) was incubated with 10  $\mu$ M of biotinylated H3K9me2 and 100  $\mu$ M of S-adenosyl methionine (Sigma), with and without 100  $\mu$ M of chaetocin (Sigma) in 50 mM Tris-HCl (pH 8.5) buffer containing 10 mM NaCl, 5 mM MgCl<sub>2</sub>, 1 mM DTT and 1 mM PMSF at 30°C. Aliquots of the reaction mixtures were sampled, diluted in TBS and immediately frozen. These samples were thawed and analyzed using ELISA as described above.

## Supplementary Material

Refer to Web version on PubMed Central for supplementary material.

## Acknowledgments

We thank K.D. Witttrup (Massachusetts Institute of Technology) for an antibody library, J. Lavinder and G. Georgiou for assistance in peptide procurement, J. Ahringer (Cambridge University) for sharing commercial antibodies, M. Gardel and Y. Beckham (University of Chicago) for a cell line and advice, A. A. Kossiakoff and M. Lugowski for access to cell culture equipment and microscopes, R. Hoey, N. Bharwani, A. Crofts and R. Ptashkin for technical assistance, and S. Nishikori for helpful discussion. We thank the University of Chicago DNA sequencing and flow cytometry core facilities, and the Institute for Genomics and Systems Biology High-throughput Genome Analysis facility. This work was supported by the National Institutes of Health grants (R21 DA025725 and RC1 DA028779 to S.K., GM085394 to B.D.S., U01 HG004264 to K.P.W., and U01 ES017154 to P.J.F.), and the University of Chicago Comprehensive Cancer Center (to S.K.).

## References

1. Strahl BD, Allis CD. *Nature*. 2000; 403:41–45. [PubMed: 10638745]
2. Kouzarides T. *Cell*. 2007; 128:693–705. [PubMed: 17320507]
3. Barski A, et al. *Cell*. 2007; 129:823–837. [PubMed: 17512414]
4. Rea S, et al. *Nature*. 2000; 406:593–599. [PubMed: 10949293]
5. Egelhofer TA, et al. *Nat. Struct. Mol. Biol.* 2011; 18:91–93. [PubMed: 21131980]
6. Fuchs SM, Strahl BD. *Epigenomics*. 2011; 3:247–249. [PubMed: 22122332]
7. Nishikori S, et al. *J. Mol. Biol.* 2012; 424:391–399. [PubMed: 23041298]
8. Cobaugh CW, Almagro JC, Pogson M, Iverson B, Georgiou G. *J. Mol. Biol.* 2008; 378:622–633. [PubMed: 18384812]
9. Feldhaus MJ, et al. *Nat. Biotechnol.* 2003; 21:163–170. [PubMed: 12536217]
10. Weiss GA, Watanabe CK, Zhong A, Goddard A, Sidhu SS. *Proc. Natl. Acad. Sci. U.S.A.* 2000; 97:8950–8954. [PubMed: 10908667]
11. Fuchs SM, Krajewski K, Baker RW, Miller VL, Strahl BD. *Curr. Biol.* 2011; 21:53–58. [PubMed: 21167713]
12. Bulut-Karslioglu A, et al. *Nat. Struct. Mol. Biol.* 2012; 19:1023–1030. [PubMed: 22983563]
13. Blahnik KR, et al. *PLoS One*. 2011; 6:e17121. [PubMed: 21347206]
14. Bernstein BE, et al. *Cell*. 2005; 120:169–181. [PubMed: 15680324]
15. Tan M, et al. *Cell*. 2011; 146:1016–1028. [PubMed: 21925322]
16. Zheng Y, et al. *Proc. Natl. Acad. Sci. U.S.A.* 2012; 109:13549–13554. [PubMed: 22869745]
17. Greiner D, Bonaldi T, Eskeland R, Roemer E, Imhof A. *Nat. Chem. Biol.* 2005; 1:143–145. [PubMed: 16408017]
18. Quinn AM, Simeonov A. *Curr Chem Genomics*. 2011; 5:95–105. [PubMed: 21966349]
19. Haque A, Andersen JN, Salmeen A, Barford D, Tonks NK. *Cell*. 2011; 147:185–198. [PubMed: 21962515]
20. Sidorin EV, Solov'eva TF. *Biochemistry. Biokhimiia*. 2011; 76:295–308. [PubMed: 21568864]
21. Chao G, et al. *Nat. Protoc.* 2006; 1:755–768. [PubMed: 17406305]
22. Ackerman M, et al. *Biotechnology progress*. 2009; 25:774–783. [PubMed: 19363813]

23. Wojcik J, et al. *Nat. Struct. Mol. Biol.* 2010; 17:519–527. [PubMed: 20357770]
24. Fellouse FA, et al. *J. Mol. Biol.* 2007; 373:924–940. [PubMed: 17825836]
25. Zhang X, et al. *Proc. Natl. Acad. Sci. U.S.A.* 2012; 109:8534–8539. [PubMed: 22586122]
26. Lehnertz B, et al. *Curr. Biol.* 2003; 13:1192–1200. [PubMed: 12867029]
27. Ruthenburg AJ, et al. *Cell.* 2011; 145:692–706. [PubMed: 21596426]
28. Frieze S, O'Geen H, Blahnik KR, Jin VX, Farnham PJ. *PLoS One.* 2010; 5:e15082. [PubMed: 21170338]
29. O'Geen H, Echipare L, Farnham PJ. *Methods Mol. Biol.* 2011; 791:265–286. [PubMed: 21913086]
30. Negre N, et al. *Nature.* 2011; 471:527–531. [PubMed: 21430782]
31. Shechter D, Dormann HL, Allis CD, Hake SB. *Nat. Protoc.* 2007; 2:1445–1457. [PubMed: 17545981]
32. Garcia BA, et al. *Nat. Protoc.* 2007; 2:933–938. [PubMed: 17446892]

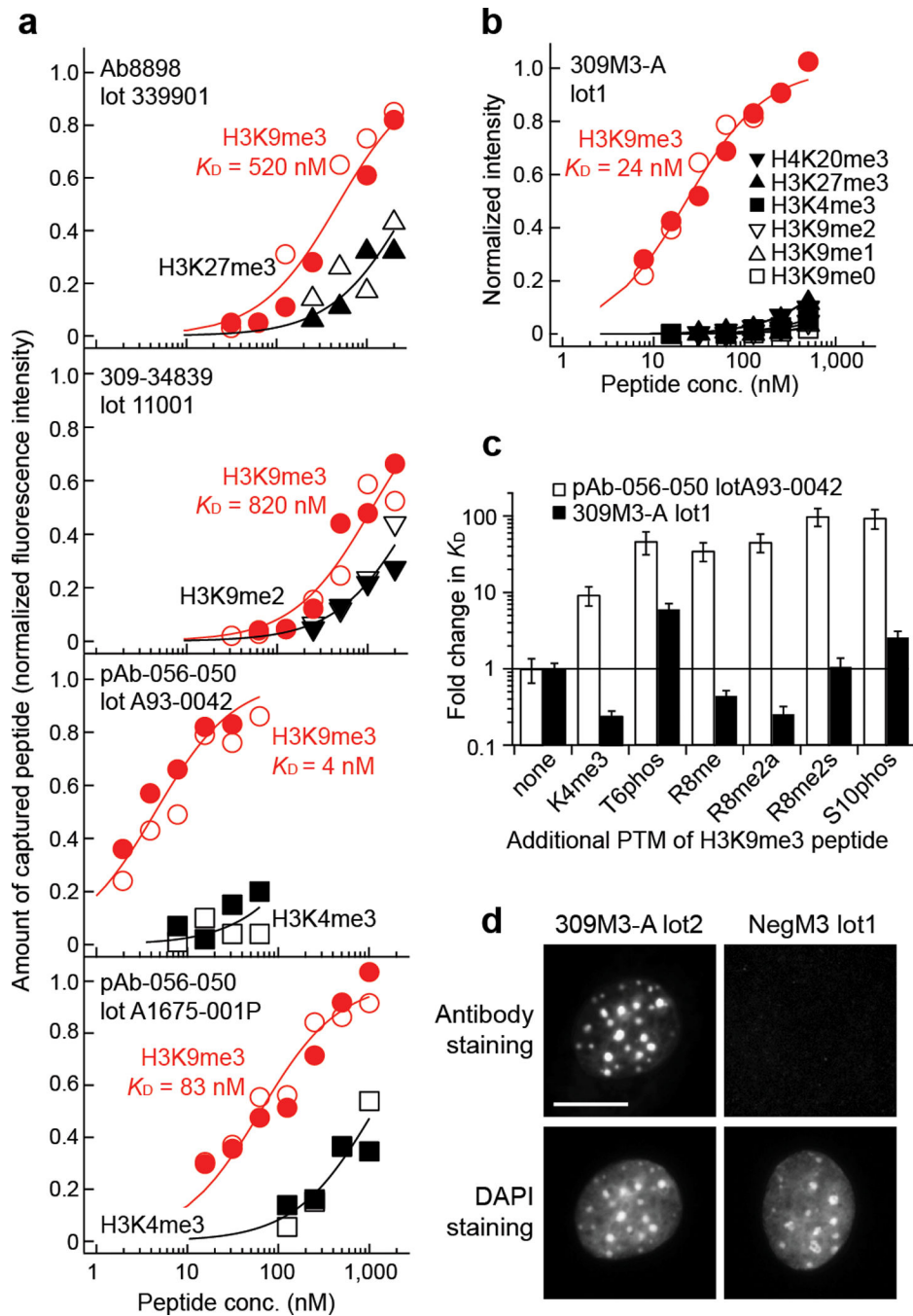


**Figure 1.** Characterization of commercial and recombinant anti-H3K9me3 antibodies. **(a and b)** Titration curves of commercial anti-H3K9me3 antibodies (b) and a recombinant antibody (c) to the H3K9me3 peptide (shown in red) and off-target peptides (in black) using the peptide IP assay ( $n = 2$ ).  $K_D$  values to H3K9me3 are shown. Only the off-target that had the highest binding is shown for clarity in **(a)**. See Supplementary Fig. 1 and 3 for the complete set of titration curves. **(c)** Influence of secondary modifications on antibody affinity. The fold changes in  $K_D$  values of indicated antibodies to the H3K9me3 peptides containing an

additional modification are shown. Errors shown are estimated from model fitting errors of each titration. Abbreviations used are: me2a, asymmetric dimethylation; me2s, symmetric dimethylation; and phos, phosphorylation. **(d)** Immunofluorescence staining of NIH 3T3 cells with 309M3-A and NegM3, the negative control Fab (top panels). The bottom panels show DAPI staining. Scale bar, 10  $\mu$ m.

Author Manuscript

Author Manuscript

Author Manuscript

Author Manuscript

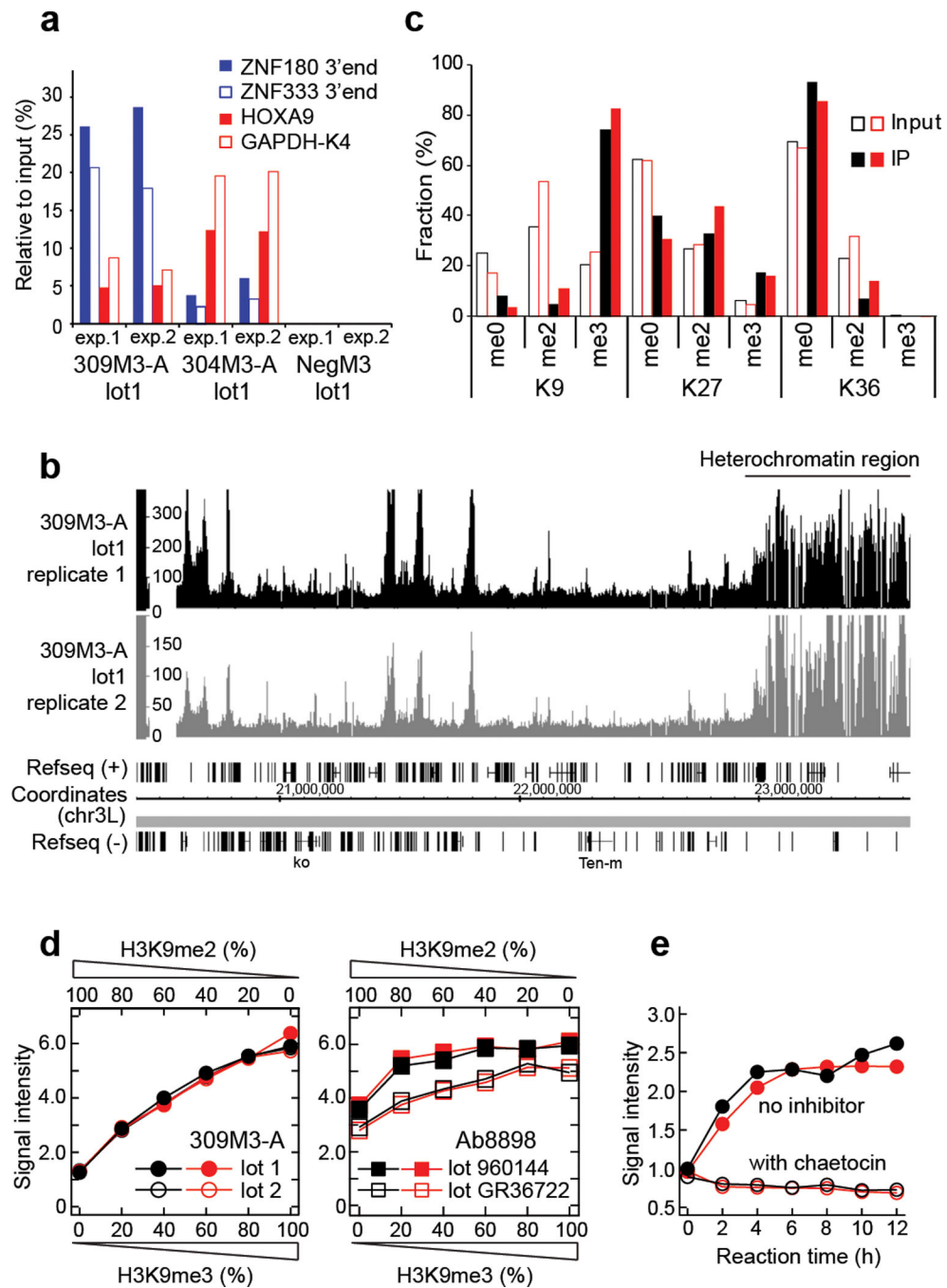


**Figure 2.** Validation and utility of high specificity of recombinant antibodies. **(a)** ChIP followed by quantitative PCR (qPCR) ( $n = 2$ ). **(b)** Biological duplicates of ChIP-seq of *D. melanogaster* embryos performed with 309M3-A lot1. The number of reads is plotted versus genomic location for a portion of chromosome 3L. **(c)** IP followed by mass spectrometry analysis of the N-terminal tail of histone H3. Summary of the fractions of PTMs at the indicated lysine residues of histone H3 before and after IP with 309M3-A are shown ( $n = 2$ ). See Supplementary Fig. 6 for detail. **(d)** Assessment of the ability of antibodies to discriminate

the H3K9me2 and H3K9me3 marks. Binding signal of the indicated antibodies to mixtures of the H3K9me2 and H3K9me3 peptides is plotted versus the ratio of the two peptides ( $n = 2$ ). (e) Detection of SUV39H1 activity using the methyltransferase assay with 309M3-A, and inhibition of the enzyme by chaetocin ( $n = 2$ ).

Author Manuscript

Author Manuscript

Author Manuscript

Author Manuscript